

**ELECTRICAL PROPERTIES OF JUNCTIONS BETWEEN ALUMINUM
AND
POLY [3-(2'-PENTYLOXY-5'-(1'''-OXOOCTYL) PHENYL)THIOPHENE]**

**A thesis Presented to the School of Graduate Studies
Addis Ababa University In Partial Fulfillment of the Requirements for
the degree of Master of Science in Physics**

**by
Hiwot Digafe**

**June 2003
Addis Ababa**

**ADDIS ABABA UNIVERSITY
SCHOOL of GRADUATE STUDIES**

**ELECTRICAL PROPERTIES OF JUNCTIONS BETWEEN ALUMINUM
AND
POLY [3-(2'-PENTYLOXY-5'-(1'''-OXOOCTYL)PHENYL)THIOPHENE]**

by

Hiwot Digafe

Department of Physics

Faculty of Science

APPROVED BY THE EXAMINATION COMMITTEE

Name

Signature

Dr. Bantikassegn Workalemahu, Advisor

Prof. Sharma S. K., Examiner

Prof. Singh P., Examiner

Declaration

I declare that the thesis is my original work, has not been submitted for a degree in any other University and that all sources of material used for the thesis have been duly acknowledged.

Name: Hiwot Digafe

Signature: _____

Place and date of submission: Addis Ababa University

Department of Physics

June 2003

This thesis has been submitted for examination with my approval as University advisor.

Name: Dr. Bantikassegn Workalemahu

Signature: _____

Date: _____

Acknowledgement



I would like to express my sincere thanks to my advisor, Dr. Bantikassegn Workalemahu, for introducing me to the field of conjugated polymer, scientific guidance, encouragement and unlimited support during the time of work. The convenient working environment with well-equipped laboratory he has created with the necessary journals and materials are greatly acknowledged.

I also indebted to my family for their solidarity, inspiration and unlimited support for the time I have spent in the university instead of doing job.

I would like to express my sincere thanks to the International Program in the Physical Sciences (IPPS) Uppsala University for equipping a research laboratory with all the necessary materials.

Special thanks also goes to the department of physics, Addis Ababa University.

Finally, I would like to express my sincere thanks to:

-  Ato Abrar Sherif for his support and encouragement.
-  All my colleagues who helped me one way or another.

Abstract

This thesis is based on the study of the electronic properties of Junction between Al and poly[3-(2'-pentyloxy-5'-(1'''-oxoocty)phenyl)thiophene in the form of Al/poly[3-(2'-pentyloxy-5'-(1'''-oxoocty)phenyl)thiophene]/ITO sandwich structure. The junction between aluminium contacts to poly[3-(2'-pentyloxy-5'-(1'''-oxoocty)phenyl)thiophene films was studied using current-voltage, capacitance-voltage and complex impedance spectroscopy techniques. The current density-voltage curve is asymmetric and non-ohmic and shows Schottky barrier type rectification. The complex impedance spectra are semi-circles that show the existence of a region depleted of mobile charge carriers. An equivalent circuit consisting of one parallel RC circuit is envisaged as a model of the interface.

TABLE OF CONTENTS

1. INTRODUCTION.....	1
2. CONJUGATED POLYMERS.....	3
2.1 CONDUCTING POLYMERS	3
2.2 HYBRIDIZATION	5
2.2.1 Hybridization Of Carbon.....	7
2.3 PEIERLS DISTORTION	8
2.4 PEIERLS DISTORTION IN POLYACETYLENE.....	10
3. ELEMENTARY EXCITATION AND CHARGE TRANSPORT MECHANISM.....	13
3.1 CONJUGATIONAL DEFECT	13
3.1.1 Solitons.....	14
3.1.2 Polarons And Bipolarons.....	15
3.2 CHARGE TRANSPORT MECHANISM	18
3.2.1 Hopping And Variable Range Hopping.....	19
3.2.2 Mobility And Conductivity.....	21
4. ELECTRICAL PROPERTIES OF METAL-POLYMER CONTACTS... 	23
4.1 METAL-SEMICONDUCTOR CONTACT.....	23
4.2 CURRENT-VOLTAGE CHARACTERISTICS.....	25
4.3 IMPEDANCE SPECTROSCOPY.....	27
4.4 CAPACITANCE-VOLTAGE RELATION	32
5. EXPERIMENT.....	34
5.1 ABSORPTION SPECTRUM MEASUREMENT.....	34
5.2 CURRENT-VOLTAGE MEASUREMENT.....	34
5.3 COMPLEX IMPEDANCE MEASUREMENT.....	37
5.4 CAPACITANCE-VOLTAGE MEASUREMENT	37
6. RESULTS AND DISCUSSION.....	38
6.1 ABSORPTION SPECTRUM	38
6.2 CURRENT-VOLTAGE CHARACTERISTICS	39
6.3 COMPLEX IMPEDANCE ANALYSIS	42
6.4 CAPACITANCE-VOLTAGE CHARACTERISTICS.....	45
7. CONCLUSION.....	48

List of Figures	page
2.1 Basic chemical structure of some of the conjugated polymers.....	4
2.2 Energy schematics showing the overlap of the 1s atomic orbitals of two H atoms to form a bonding and antibonding molecular orbital.....	5
2.3 Cylindrically symmetrical σ -bonding of a hydrogen molecule	6
2.4 Overlap of two p atomic orbitals to give a bonding π -MO.....	6
2.5 (a) Metallic system of a linear arrangement (b) a linear semiconducting dimerized system with a band gap and the Fermi level.....	9,10
2.6 The energy band structure of trans-polyacetylene for equal bond length and alternating bond length, respectively.....	12
3.1 A Transition region (soliton) created by two different bond-alternating phases A and B.....	13
3.2 Schematics of the band diagram of polyacetylene with solitons. Changed solitons do not carry spin, while neutral solitons have spin $S=1/2$	15
3.3 Two non-degenerate forms of polythiophene (a) aromatic form and (b) quinoidal form	16
3.4 Motion of a soliton in Polythiophene.....	17
3.5 Formation of a polaron (a) and a bipolaron (b) in polythiophene.....	17
3.6 Energy band diagrams of positive polaron and positive bipolaron and possible transitions of charge carriers.....	18
3.7 The densities of states for non-crystalline solids near a gap	22
4.1 Metal-Semiconductor energy band diagram (a) before contact (b) after contact.....	24

4.2	Band diagrams for p-type semiconductor-metal contact for (a) $\phi_m > \phi_s$, which is ohmic and (b) $\phi_m < \phi_s$, which is rectifying contact.....	25
4.3	Four basic transport process under forward bias Schottky barrier diode.....	26
4.4	Parallel RC circuit	28
4.5	Cole-Cole plot of parallel RC circuit	29
4.6	Circuit for a contact resistance R_C connected in series with parallel RC circuit (a) and its Cole-Cole plot (b).....	30
4.7	An equivalent RC circuit of Metal-Insulator-Semiconductor device	31
4.8	Idealized Cole-Cole plots for the circuit shown in Fig 4.7.....	31
5.1	Preliminary steps in preparing the device.....	35
5.2	Chemical structure of the polymer and the sandwich Al/ poly[3-2'- pentyloxy-5'(1''-oxoocty)phenyl]thiophene/ITO-glass photodiode.....	36
6.1	Absorption spectrum of poly[3-(2'-pentyloxy-5'(1''-oxoocty)phenyl) thiophene].....	39
6.2	(a) Current density (J) Voltage (V) characteristics (b) logJ-V for poly[3-2'- pentyloxy-5'(1''-oxoocty)phenyl]thiophene	39,41
6.3a	Cole-Cole plot of Al/poly[3-(2'-pentyloxy-5'(1''-oxoocty)phenyl) thiophene]/ITO sandwich structure.....	42
6.3b	Cole-Cole plot of different biasing Voltage	44
6.4a	The graph of C^{-2} versus V for poly[3-(2'-pentyloxy-5' (1''oxoocty)phenyl]thiophene].....	46
6.4b	Linear fit for the selected region of the C-V plot.....	47

List of Tables

page

6.1 Parameters extracted from Fig. 6.2.....42

6.2 Parameters obtained from Fig. 6.3.....45

1. Introduction

A polymer is a chain of monomers, which are connected by covalent bonds that form a polymer backbone so polymers are long chain organic molecules of very high molecular weight. Therefore, these molecules are called macromolecules. While the exact molecular weight that is required for an organic molecule to be called a polymer is a subject of continued debate, often polymer scientists put the number above 25,000g/mol [1]. This is the minimum molecular weight required for good physical and mechanical properties for many important polymers.

For a long time, polymers were considered good insulators and were widely used as insulating materials. However, this concept has been radically changed since MacDiarmid's group with the participation of Shirakawa showed in 1977 that the conductivity of PA can be increased via doping by 13 orders of magnitude up to 10^3 - 10^4 S/cm i.e. $(\text{Ohm-cm})^{-1}$ this value is comparable to the conductivity of some metals. This discovery was a turning point in the studies of conducting polymers [2].

In 1977 shirakawa, Heeger, Macdiarmid discovered that polyacetylene doped with iodine worked as a conductor [3] this discovery paved way for a new field of conducting and semiconducting polymer materials. When the Cavendish group at Cambridge University discovered that semiconducting polymers could exhibit electro luminescence [4] a surge towards polymer electronics was taken. New tentative applications such as light emitting diodes (LEDS) [5], lasers [6], solar cells [7], and photodiodes [8] saw the break of dawn. Other applications such as polymeric actuators (micro muscles) [9] and transistors [10] have also been devised.

The above applications are a selection of possible devices based on the conductive and semi conductive properties of conjugated polymers. Plastic materials may not compete with silicon technology in terms of building fast electronics, but are attractive from a point of low-cost disposable electronics, as well as in display technology. Some attractive properties, in comparison to standard inorganic devices, of plastic electronics are lower cost, simpler packaging, and the ability to use flexible substrates.

This research based on the electrical properties of junction between aluminium and Poly[3-(2'-pentylloxy-5'-(1'''-oxooctyl)phenyl)thiophene]. The sandwich structure that we made in the laboratory (here locally) on which the work has been done is of the form Al/Poly[3-(2'-pentylloxy-5'-(1'''-oxooctyl)phenyl)thiophene]/ITO diode. The absorption spectrum, current-voltage, capacitance-voltage measurement as well as the complex impedance spectroscopy are used for characterization of the above sandwich structure. We used thermionic emission theory to interpret the semi-logarithmic plot of J (current density)-V (Voltage) curve characteristics and the complex impedance is measured and plotted a Cole-Cole plot and analyzed.

2. Conjugated Polymers

The field of conjugated polymer is fairly young as is the device processing of the materials. To make use of the electrical and optical properties of these materials new techniques, as well as modified standard processing technique are used in device fabrication.

Conjugated polymers are a group of polymers that have electrical properties ranging from insulators and semiconductors in their undoped form to conductors in their doped form. In conjugated polymers carbon atoms are connected by consecutive single and double bonds, the alternating of double and single bonds is what is meant by the conjugation of the polymer. The semiconductor and conducting properties is directly related to the conjugation of the polymer backbone. In conjugated polymers the four valence electrons of carbon hybridize to form three sp^2 orbitals and one p_z orbital. The sp^2 Orbitals form strong localized bonds between atoms in a conjugated polymer, σ -bonds, while the p_z orbital form a more delocalized bond, a π -bond, between the carbon atoms of the polymer back bone. As the π -electrons is delocalized to some degree, they are free to move a certain length along the carbon, the conjugation length.

2.1 Conducting Polymers

In 1977 it was first discovered that the conductivity of polyacetylene could be increased by chemical oxidation many orders of magnitude [11,12]. Since then, it has remained of intensive research on synthetic metals technology.

There are many reasons for the popularity of conducting polymers. Among these, their promising potential for new applications, the extended systems of conjugated bonds are

subjected to quantum mechanical analysis, the similarity of solitons and solitary waves creates an interdisciplinary link to field theory and particle physics.

Organic molecules that contain double bonds show different electronic properties compared to saturated molecules, which only have single bonds. Especially in the case of alternating single and double bonds, called conjugation, the polymers manifest properties of technological interest.

The most important conducting polymers and their structures are shown in the **fig. 2.1** below.

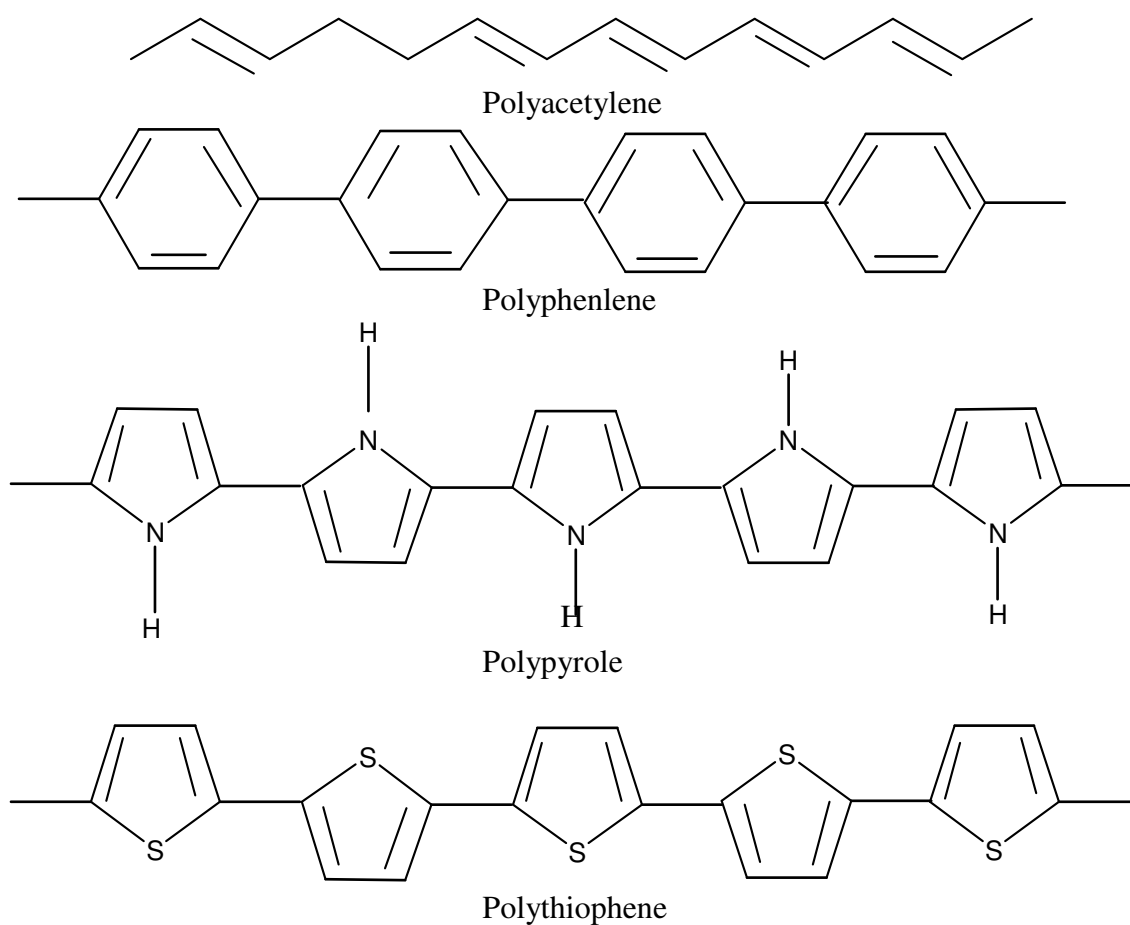


Fig.2.1 Basic chemical structure of some of the conjugated polymers.

2.2 Hybridization

Bonds in organic compounds are formed from hybrid orbitals that result from the mixing of two or more orbitals in the bonded atoms. This mixing process is called orbital hybridization. As a result of hybridization two or more hybrid orbitals can be formed from atomic orbitals that are not identical. The number of hybrid atomic orbitals created is the same as the number of atomic orbitals used in hybridization.

Heisenberg uncertainty principle and the Pauli exclusion principle, is the basis for understanding the formation of atomic orbital [13]. The atomic orbital, for instance, the 1s orbitals of two hydrogen atoms, form a molecular orbital (MO) if they are brought close enough so that they overlap. There are two possible ways in which the wave function of the electrons in both hydrogen atoms superposes. One of these MOs is of significantly lower energy than the sum of the energy of the original atomic orbital. It is known as a bonding MO the other orbital, called an anti-bonding MO, is of higher energy than the original atomic orbital. Energetically the former gives stable hydrogen molecules, while the latter needs an expenditure of external energy.

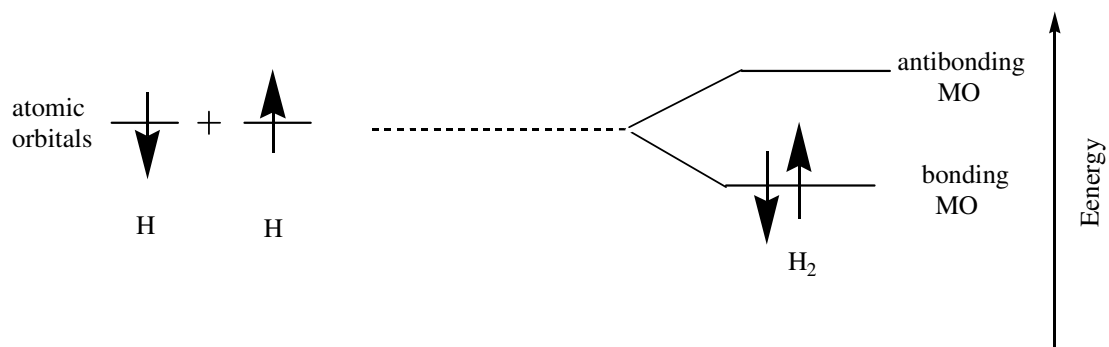


Fig. 2.2 Energy schematics showing the overlap of the 1s atomic orbitals of two H atoms to form a bonding and antibonding molecular orbital.

As the molecular orbital do an atomic orbital contain no more than two electrons. When a covalent bond is formed, the two electrons originally in the atomic orbital of the separation atoms now go in to much lower energy bonding MO. The formation of a covalent bond involves the sharing of only two electrons i.e. the pair that can be accommodated in the bonding molecular orbital. Two different cylindrically symmetrical about a line joining the two nuclei involved is called σ -orbital, and the bonds formed are called σ -bonds.

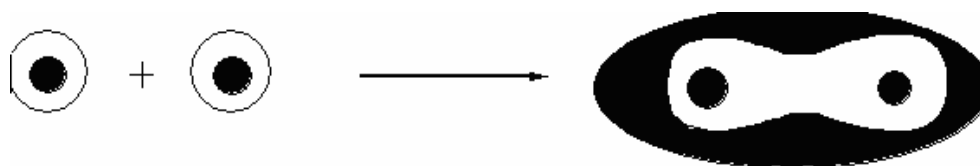


Fig. 2.3 Cylindrically symmetrical σ -bonding of a hydrogen molecule.

A second type of covalent bond can be formed by the overlap of two atomic 2p orbital as shown in **fig. 2.4** below. This bonding MO is not cylindrically symmetrical about a line joining the two nuclei. It is called a π -bonding molecular orbital. The resultant covalent bond is called a π -bond.



Fig.2.4 Overlap of two p atomic orbitals to give a bonding π MO.

2.2.1 Hybridization Of Carbon

Hybridization of atomic orbitals is of fundamental importance in understanding the nature of covalent bonds. Standard, insulating organic polymers have saturated (sp^3 hybrid) carbons making up their backbones. In organic conjugated polymers, the backbones consist of sp^2 -hybridized carbons. This electron configuration results in three σ -bonding electrons, the 2s, $2p_x$ and $2p_y$ electrons, and a remaining $2p_z$ electron form a π -bond. Two adjacent $2p_z$ orbitals can overlap, forming a π -bond. In a conjugated polymer, the $2p_z$ electron orbitals overlap along the backbone, which gives rise to the delocalization of the π -electron system. The π -bands thus formed becomes dispersed due to the delocalized nature of the π -electronic orbitals. Of course, one also has the case where the $2p_z$ electron orbitals do not overlap along the backbone (being orthogonal to each other), and in that case the resulting π -bands are flat, i.e. showing no dispersion.

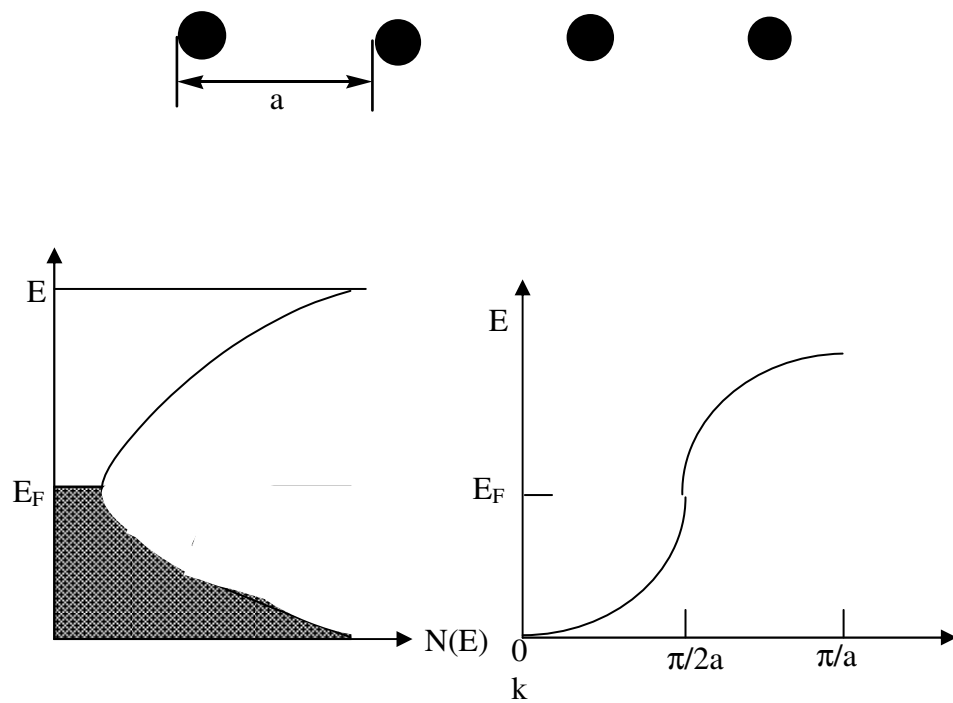
For instance, in methane (CH_4) in which a carbon atom forms covalent bonds with the four hydrogen atoms the carbon atom does not employ its 2s and 2p orbitals as they are found in an isolated atom. Instead more stable covalent bonds are formed if these four orbitals are combined to form hybrid orbitals directed towards the corner of a regular tetrahedron. They are called sp^3 hybrid orbitals, because they are formed from one 2s and three 2p atomic orbitals. In methane the overlap of one of the sp^3 hybrid orbitals with this atomic orbitals of a hydrogen atom forms a sigma MO and a covalent C-H bond. Such single covalent bond formation uses sp^3 hydride orbitals.

The nature of orbital hybridization has a significantly impact on the structures of polymers. Organic polymers having sp^3 hybridization are bound to form sigma (σ) bonds only. Consequently the separation between bonding (HOMO- Highest Occupied MO, or valence band) and anti bonding (LUMO- Lowest Unoccupied MO, or conduction band) is large. The localized states end up having a large energy gap (E_g). On the other hand, the sp^2 hybridization having π -bonds in addition to the σ -bonds yields smaller separation between the bonding (π) and anti bonding (π^*) states, and hence smaller energy gap (E_g). This class of polymers, by virtue of having a combination of both σ and π -bonds, can be categorized in to two forms, namely those with localized and de-localized electronic states, respectively. The polymers with delocalized electronic configuration are capable of being doped to high electrical conductivity.

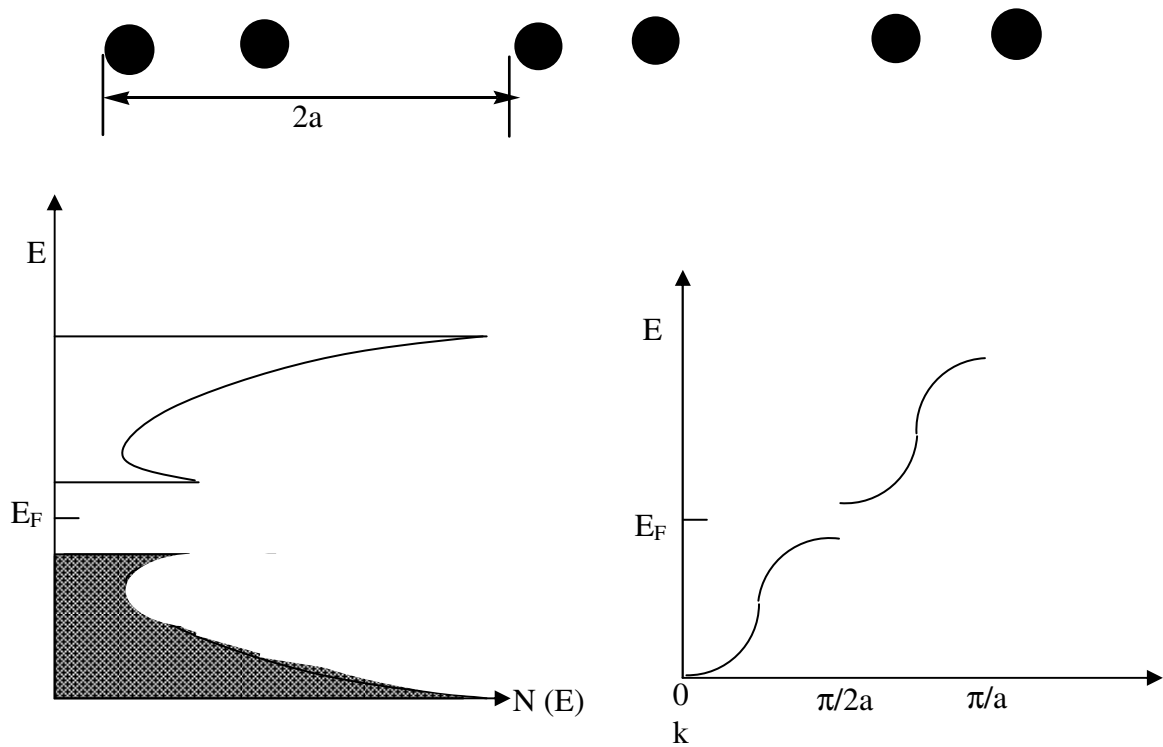
2.3 Peierls Distortion

Peierls distortion is an important case of electron lattice coupling. To understand the basic principle consider a linear arrangement of a theoretical system with one delocalized electron per unit cell see the **fig. 2.5** below. According to the Pauli principle another delocalized electron with opposite spin can be place in the unit cell and thus the unit cell is half-filled. There is no band gap in the system so it works as a conductor. Commonly, conjugated polymers are arranged in a similar manner but are not conducting in their undoped state; instead they are found in a semiconducting state with a band gap. The band gap originates from an effect sometimes referred to as peierls distortion [14]. In metallic state the π electrons of the carbon backbone will delocalized all over the carbon backbone. In this case the length of the unit cell will be the distance, a , between adjacent carbon atoms of the backbone and there will be one electron in the first Brillouin zone resulting in a half-filled band. In

conjugated polymers the polymer chain can decrease its energy by reorganization of its bond structure. Introducing a decrease in distance, σ , between the double bonds giving a dimerized structure with alternating short and long bonds decrease the energy of the chain. As this system has a lower energy compared to the equidistantly spaced system it is more liable to be found in this state. The unit cell of this system will span two carbon atoms, where each of the carbons will supply one electron resulting in a filled unit cell. A band gap will show up at the Brillouin zone boundary, creating a valence band and a conduction band, giving rise to a semi conducting behavior.



(a)



(b)

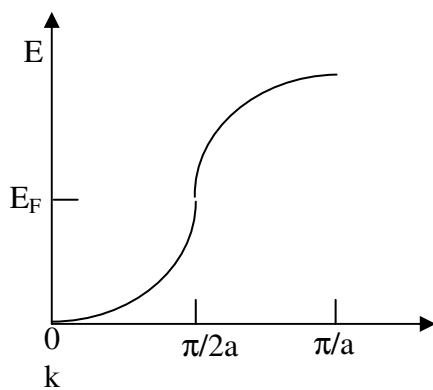
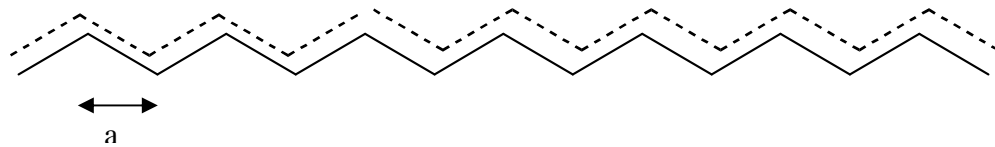
Fig. 2.5 (a) Metallic system of a linear arrangement. (b) A linear semiconducting dimerized system with a band gap and the Fermi level, the chemical potential for a semiconductor [15] a midgap.

2.4 Peierls Distortion In Polyacetylene

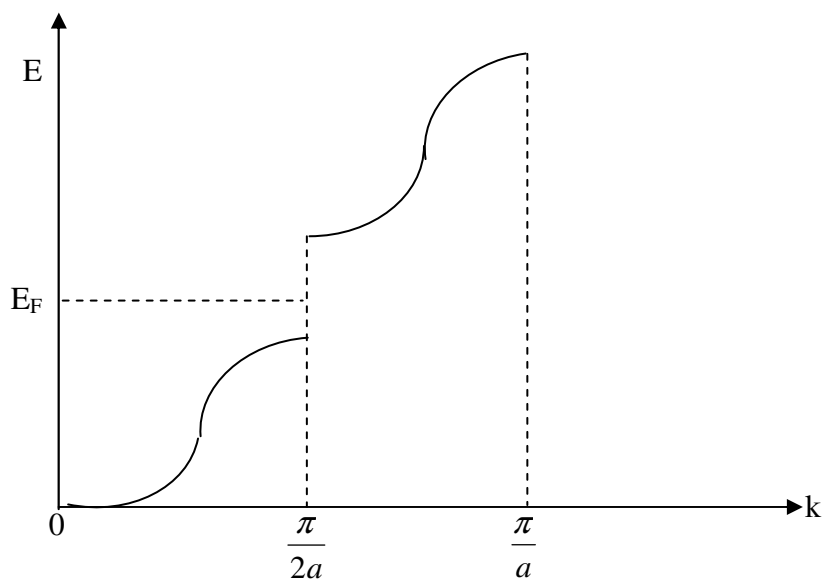
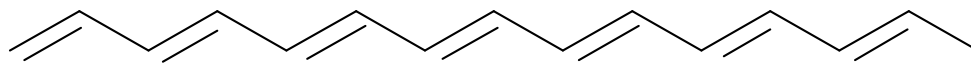
Conjugated polymers can be divided in to two groups. They are degenerate ground state polymers such as trans-Polyacetylene, and non-degenerate ground state polymers such as poly (p-phenylenevinylene).

Trans-polyacetylene is often used when describing various properties of conjugated polymer in general and degenerate ground state polymer in particular due to its simple geometric and

electronic structure. As can be seen **fig. 2.6a** trans-polyacetylene consist of repeating segment of C-H groups. If the C-C bonds along the chain axis were all of the same length trans-polyacetylene would be a quasi-one-dimensional metal due to the half-filled valence π -band. This is not the case in trans -polyacetylene however since peierls distortion and e-e correlation effect contribution to dimerization of the lattice [14] i.e. the C-C bonds of the polymer back bond alternate between single and double bond-type character. These will double the size of the unit cell from one C-H unit to two, which reduce the Brillouin zone to half its previous size, as show in **fig. 2.6b** below. The energy bands are thus folded back in to the first Brillouin zone and an energy gap, E_g , is opened up at the zone edge with the Fermi level E_f residing in the middle of the gap between the valence and the conduction band per definition. This transformation changes the polymer in to a semiconductor.



(a)



(b)

Fig.2.6 The energy band structure of trans-Polyacetylene (a) for equal bond length
And (b) alternating bond length, respectively.

3. Elementary Excitation And Charge Transport Mechanism

In conjugated polymers electrons and holes are strongly associated with the lattice, in which they move in. They exist as quasi-particles [13] in the form of solitons, Polarons, and bipolarons. In general polymers have non-degenerate ground states. In a non-degenerate polymer the energy of the chain will be dependent on the type of bond geometry. Trans-polyacetylene is a polymer with a degenerate ground state.

3.1 Conjugational Defect

The ground state geometry of trans-polyacetylene is degenerate since the order in which the C-C single and double bonds alternate leads to the same ground state energy. This in turn means that the ground state energy also is degenerate with the polymer having two possible bond alternation patterns as shown in **fig. 3.1** below. For such systems, so-called "bond alternation defects" can occur i.e. the order of C-C single and double bonds are changed over a finite length of the polymer chain creating a transition region where the bond is suspended with the bonds being roughly of the same length see the **fig. 3.1** below.

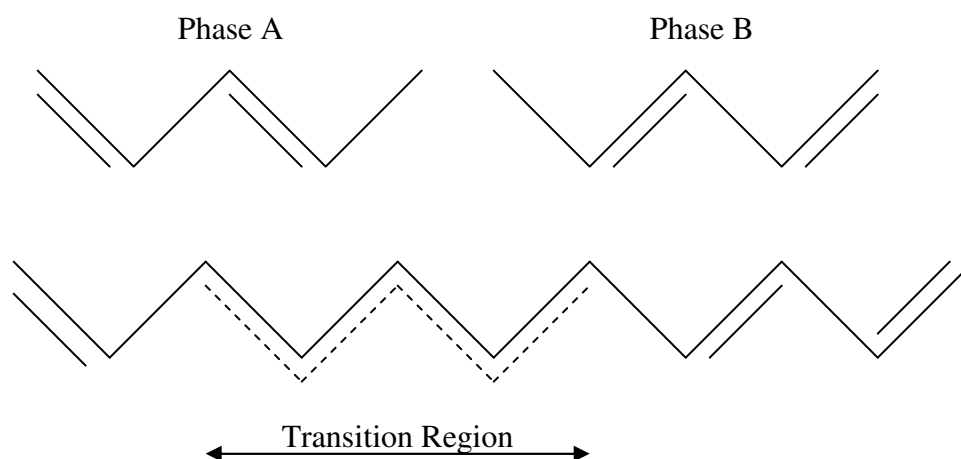


Fig.3.1 A Transition region (soliton) created by two different bond-alternating phases A and B

A bond alternation defect (transition region) with thus causes the isolation of unpaired electron. This type of defects is called solitons. Since the polymer remains neutral the soliton behave like charge-less unpaired spin-carriers [16,17].

3.1.1 Solitons

The cause of energy gap formation is uninterrupted double bond and single bond alternation. However, at the misfit (soliton site) the bond alternation is interrupted. At the bonding; rather it forms a nonbonding state that lies in the middle of energy gap.

There are neutral as well as positively or negatively charged solitons. The valance (π) and the conduction (π^*) bands, and the soliton mid-gap state maybe empty or can be occupied by charge carriers.

Solitons are always created in pairs forming a soliton and an antisoliton. These pairs can be separated with the individual solitons moving freely along the polymer chain since the two bond alternation conformations are equal in energy.

The soliton corresponding in the electronic structure to a localized state in the middle of the band gap see **fig.** 3.2 below. The neutral soliton (S^0) has a spin of 1/2. Solitons can be formed through photo absorption as well as doping induced charge transfer. In the latter case, the soliton are either negatively charged (S^-) or carry positive charge (S^+). Note that both of the solitons are spineless charge carriers. If enough soliton pairs form be it by doping or some other process the soliton being to overlap and form an energy band [18].

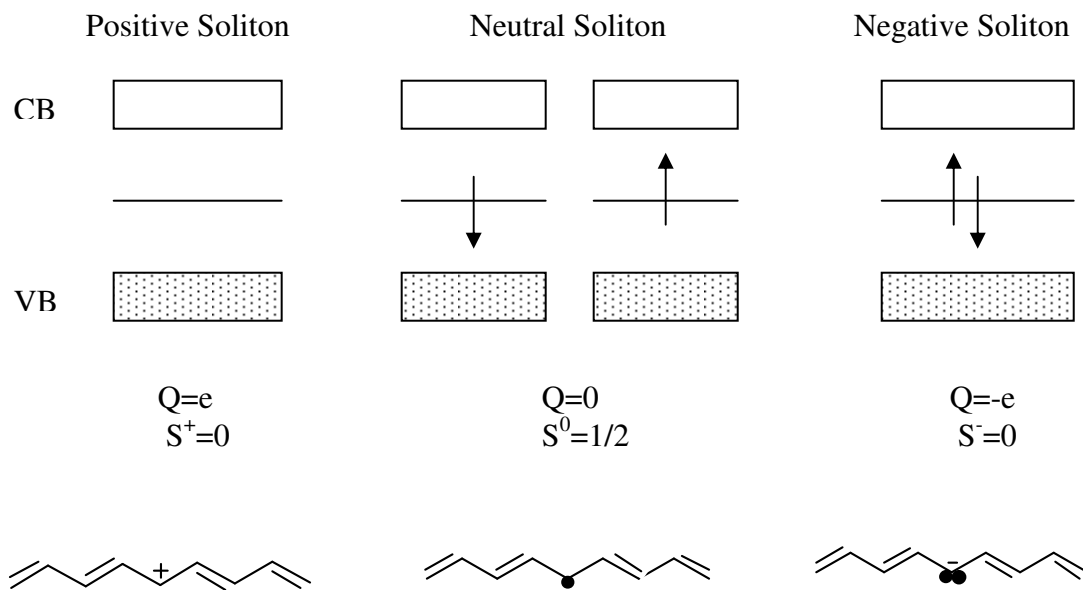


Fig. 3.2 Schematics of the band diagram of polyacetylene with solitons. Charged solitons do not carry spin, while neutral solitons have spin $S=1/2$.

3.1.2 Polarons And Bipolarons

In conducting polymers the term polaron is used to denote a localized electron state with accompanying lattice distortion. In a sense, it is a bound state of the soliton and anti soliton qualitatively, they are rather similar to when an electron moves in an ionic crystal, its surrounding medium will be polarized with negative ions being repelled away and positive ions being attracted towards it. The relative motion of the opposite ions gives rise to a polarization field is called polaron, like other elementary excitations polarons play the role of building blocks of the low lying excited in ionic crystals and polaron semiconductors. It is generally accepted to distinguish small polarons in which the electron-phonon coupling is very strong, the polaron size is comparable or even smaller than the lattice constant from Polarons for which the coupling is relatively weak, and the size is large [2].

Polyacetylene has both degenerate and non-degenerate ground states. However, many other conjugated polymers have non-degenerate ground states. The **fig. 3.3** below shows the two forms of non-degenerate polythiophene.

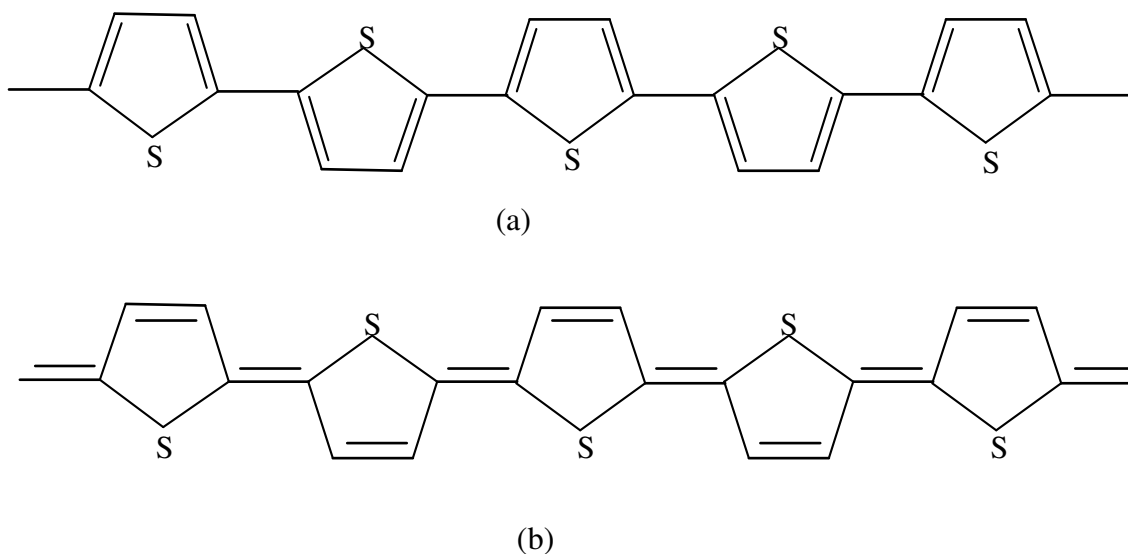


Fig. 3.3 Two non-degenerate forms of polythiophene (a) aromatic form and (b) quinoidal form.

The aromatic form has the lowest energy state and the quinoidal form has the highest energy state. In polythiophene the soliton separates the aromatic (low energy) region from a quinoidal (high energy) region. The soliton will be driven to the chain end, and changing the high energy quinoidal rings into low energy aromatic rings as it moves as depicted in the **fig. 3.4** below. Therefore, solitons in non-degenerate polymers are energetically unstable.

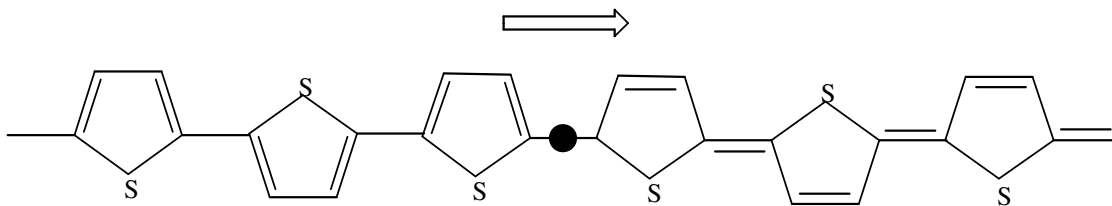
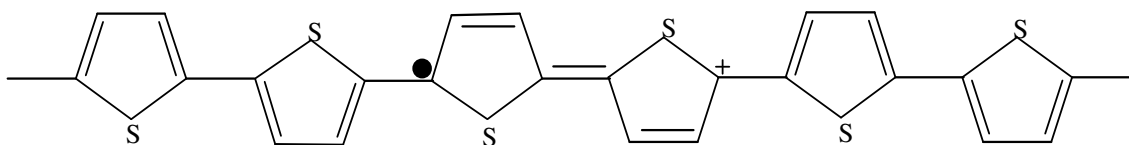
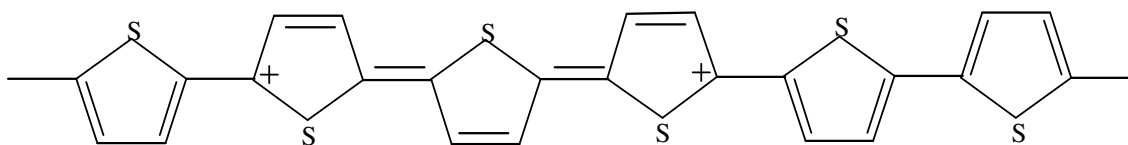


Fig. 3.4 Motion of a soliton in polythiophene.

If defects in non-degenerate ground state polymers are to be stable, bound double defects must be created. Singly charged states are called Polarons and doubly charged states are called bipolarons. These are shown in **fig. 3.5** (a), and (b) respectively.



(a)



(b)

Fig. 3.5 Formation of a polaron (a) and a bipolaron (b) in polythiophene.

Polarons can be injected by a metal electrode but can also be created by light excitation. For light excitation the mechanism of charge generation may be either by direct polaron excitation [19,20] and/or generation may be an intrachain event or an interchain event.

A polaron is characterized by two states in the gap. The emergence of two states can be rationalized to occur through interaction between the mid-gap states belonging to the soliton components of polaron. New electronic states are created in the energy gap when oxidizing a non-degenerate ground state polymer. The schematics of the energy band diagram for both polaron and bipolaron are shown in the **fig. 3.6** below.

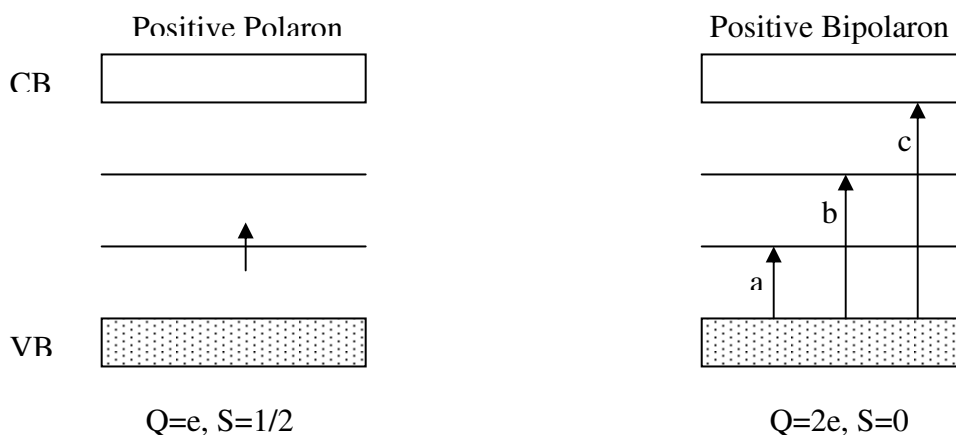


Fig. 3.6 Energy band diagrams of positive polaron and positive bipolaron and possible transitions of charge carriers.

3.2 Charge Transport Mechanism

The conduction mechanism of electrically conducting polymer has been widely investigated with polyheterocycles such as polypyrrole, polyacetylene and poly (3-hexylthiophene). In actual conjugated polymers charge carriers do not only hop along the chain but also hop across the inter chain.

In a pure respect temperature dependence of electrical conductivity is important. In a pure undoped state, conjugated polymers have a very low electrical conductivity, which can be explained by small thermal excitation of charge carriers over the band gap. However, the conductivity can increase drastically by doping.

Charge transport mechanism of undoped or lightly doped conjugated polymers can be explained by hopping (phonon-assisted quantum mechanical tunneling) mechanism between the localized solitonic, polaronic or bipolaronic states. These states below E_F are occupied and those above are empty except in case of thermal excitation. Electrons will hop from occupied to empty states.

3.2.1 Hopping And Variable Range Hopping

At very low doping levels, the conductivity is mainly due to hopping (an abbreviation for "phonon assisted quantum mechanical tunneling "). Hopping charge carriers are intermediate between trapped and free carriers [21,22] in that they spend most of the time in localized states. They are subject to relatively small thermal vibrations, but occasionally they make a big jump or hopping transition to some neighboring localized sites.

If the conduction process is due to hopping between localized state around the Fermi level, the conductivity is proportional to the number of electrons $2KT_N(E_F)$ and the probability of hopping between sites at distance R as given by

$$v_{hop} = v_{ph} \exp\left\{-2\alpha R - \frac{\omega \pm eRF}{KT}\right\} \quad 3.1$$

where the exponent $\exp(-2\alpha R)$ is due to the wave function overlap, ω is the energy difference between sites and F the external electric field. Here plus and minus sign correspond to forward and backward hopping in the field direction to obtain the result current we have to multiply the difference and the electric charge. For weak field $eRF \ll KT$, the conductivity is given by

$$\sigma = 4e^2 R^2 v_{ph} N(E_F) \exp\left(-2\alpha R - \frac{\omega}{KT}\right) \quad 3.2$$

Depending on the degree of localization, two types of hopping are possible.

Type-1- If $\alpha R_0 \gg 1$ with R_0 as the nearest neighbor distance and the mobility edge is in the higher band, only nearest neighbor hopping is available.

Type-2- If $\alpha R_0 \cong 1$ or even less, or at very low temperature, the so-called variable range hopping (VRH) should be expected as first suggested by Mott [21].

There are two competing factors. By increasing the distance the wave function overlap reduces, but the energy difference

$$\omega = \frac{3}{4\pi R^3 N(E_F)} \quad 3.3$$

is getting smaller and smaller. By balancing these two factors, the maximum hopping rate becomes

$$v_{hop} = v_{ph} \exp\left(\frac{-B}{T^{\frac{1}{4}}}\right) \quad 3.4$$

where

$$B = B_0 \left[\frac{\alpha^3}{kN(E_F)} \right]^{\frac{1}{4}} \quad 3.5$$

and B_0 is a numerical constant of order 1.

If the conduction is due to thermal excitation to extended state, the dc conductivity is given by equation 3.9 while the ac conductivity is described by the Drude formula [2]

$$\sigma(\omega) = \frac{\sigma(0)}{1 + \omega^2 \tau^2} \quad 3.6$$

Where τ is the electron relaxation time.

If the conduction is due to thermally excited hopping between band tail states, the conductivity is

$$\sigma \approx \exp\left(-\frac{E_A - E_F + \omega}{KT}\right) \quad 3.7$$

If the conduction process is determined by electron hopping near the Fermi surface, the conductivity is given by

$$\sigma(T) = \sigma_0 \exp\left[-\left(\frac{T_0}{T}\right)^4\right] \quad 3.8$$

3.2.2 Mobility And Conductivity

It was realized that near edges of the conduction and the valence bands most states should be localized [2]. And also suggested that there should be a sharp boundary between localized and extended states. Generally, the density of states for non-crystalline solids near a gap may resemble the **fig. 3.7** below.

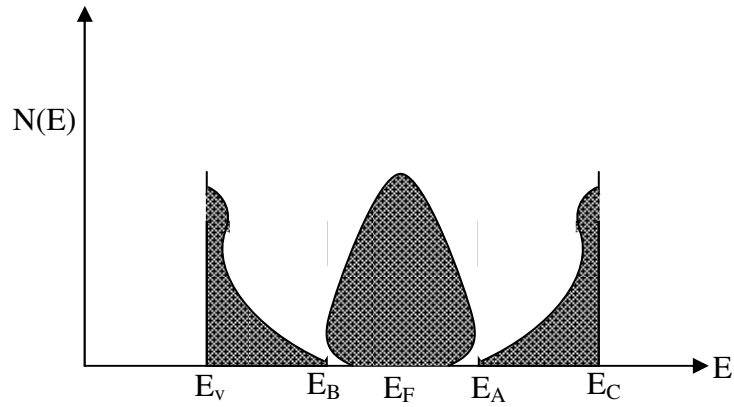


Fig.3.7 The densities of states for non-crystalline solids near a gap.

Here E_A and E_B are the band edges, while E_C and E_v are the mobility edges i.e. boundaries between localized and extended states. The localized states near the Fermi level are due to defects.

If the Fermi level is in the region of localized states, two conduction mechanisms are possible. One is the hopping process between localized states and the thermal excitation to extended states.

The conductivity given by

$$\sigma = \sigma_{\min} \exp\left\{-\frac{(E_C - E_F)}{KT}\right\} \quad 3.9$$

Where σ_{\min} is the 'minimum metallic conductivity' i.e. the lowest conductivity at absolute zero temperature if $E_F = E_C$.

4. Electrical Properties Of Metal-Polymer Contacts

Conjugated polymers have been extensively studied for their applications in electronic and opto-electronic devices such as light emitting diodes (LED), field-effect transistor (FET) and other surface junction devices. In all these applications the nature of the metallic to the polymer plays an important role [23].

4.1 Metal-Semiconductor Contact

Metal-semiconductor contacts play an important role in all kinds of solid-state devices. They are the route from the semiconductor to the outside world. The metal semiconductor junction can be either an ohmic contact or a rectifying Schottky barrier.

The work function of the metal (ϕ_m) is the amount of energy required to raise an electron from the Fermi level to a state of rest outside the surface of the metal that is called vacuum level. The work function (ϕ_s) of a semiconductor is the difference in energy between the Fermi level and the vacuum level and is also composed of bulk and surface contributions [24].

When a metal makes an intimate contact with a semiconductor, a Schottky barrier may be formed at the junction. To see how a Schottky barrier may form at the contact, consider electrically neutral metal and semiconductor, which initially are separated from each other. **Fig. 4.1** (a) and (b) show the energy band diagrams of the metal with work function greater than that of n-type semiconductor ($\phi_m > \phi_s$) before they have been brought in to contact and after contact, respectively.

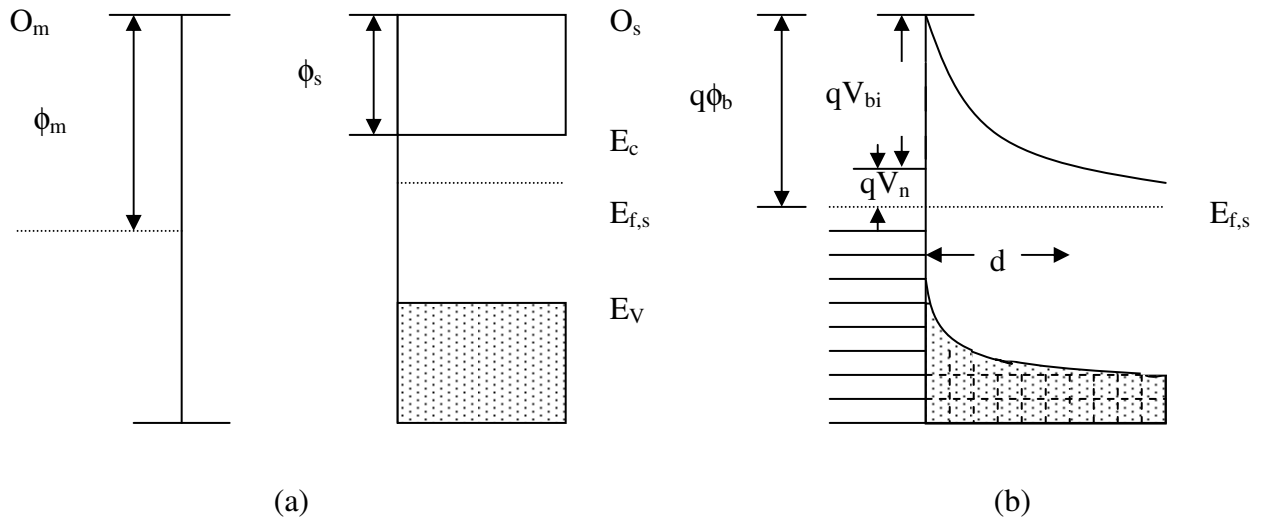


Fig. 4.1 Metal-semiconductor energy band diagram (a) before contact (b) after contact.

After the contact is made, electrons will flow out of the semiconductor into the metal until the Fermi energies $E_{F,m}$ of the metal and $E_{F,s}$ of the semiconductor coincide and a state of equilibrium is achieved [25]. A built-in potential (V_{bi}) will be established between the metal and the semiconductor.

As a result, a positive space charge through out the barrier width (d) is built up. The difference between the bottom of the conduction band, E_c , and the Fermi energy E_f in the bulk of the semiconductor is qV_n , and ϕ_b is the barrier height.

If the work function of the metal is less than that of an n-type semiconductor, the electrons shall be transported from the metal to the semiconductor setting up a negative charge in its contact layer. This leads to an increase in the free charge carrier's concentration inside the

contact layer of the semiconductor and increase its conductivity. For this reason such a layer is ohmic.

In the case of a p-type semiconductor, if $\phi_m > \phi_s$ we obtain the band diagram shown in **fig. 4.2a**, which represents ohmic contact. However $\phi_m < \phi_s$ gives rise to rectification **fig. 4.2b**.

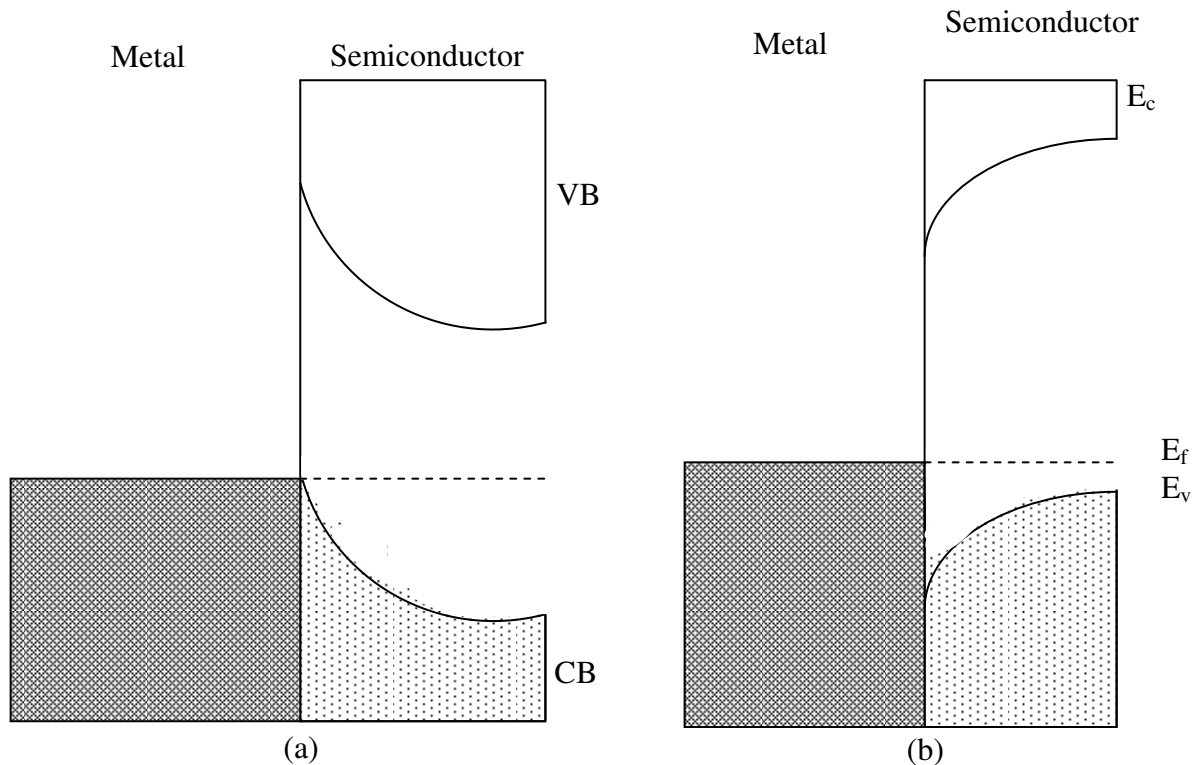


Fig. 4.2 Band diagrams for p-type semiconductor-metal contact for (a) $\phi_m > \phi_s$, which is ohmic and (b) $\phi_m < \phi_s$, which is a rectifying contact.

4.2 Current–Voltage Characteristics

Electrons and holes can be transported across a metal-semiconductor junction in various ways under an applied bias. These are (a) emission of electrons from the semiconductors over the top of the barrier in to the metal (the dominant process for Schottky diodes with moderately doped semiconductor), (b) quantum mechanical tunneling through the barrier (important for

heavily doped semiconductors and responsible for most ohmic contacts), (c) recombination in space charge region, and (d) recombination in the neutral region [26].

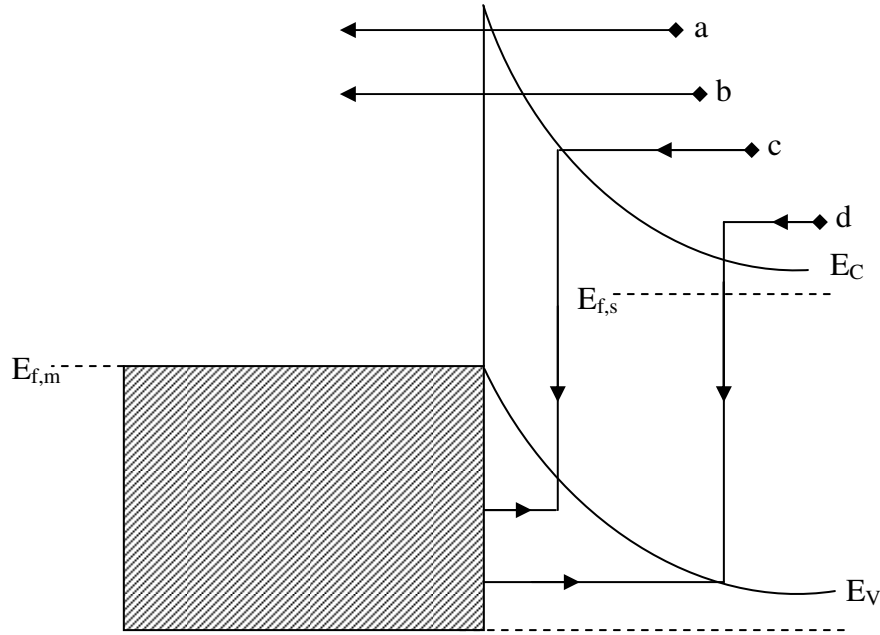


Fig. 4.3 Four basic transport processes under forward bias Schottky barrier diode

For ideal metal-semiconductor-rectifying contact, the transport equation can be given by Schottky barrier diode equation.

$$J = J_0 \left[\exp\left(\frac{qV}{nKT}\right) - 1 \right] \quad 4.1$$

where

$$J_o = A^{**} T^2 \exp\left(-\frac{q\phi_b}{KT}\right) \quad 4.2$$

where J is the total current density, J_o is the reverse saturation current density, q is the charge of an electron, V is the applied forward bias voltage, K is Boltzman constant, T is absolute temperature, n is diode ideality factor, ϕ_b is barrier height and A^{**} is modified Richardson

constant which expresses the number of electrons at the semiconductor–metal interface that may be injected in to the metal. A^{**} also takes into account the effective density of states in the conduction band. For organic semiconductor Schottky diodes the modified Richardson constant is assumed to be that of a free electron, namely, $A^{**} = 120 \text{ A/cm}^2$ [26,27].

The Schottky diode equation 4.1 can be studied under three different conditions:

1. If $J \gg J_0$, the contact will effectively block current flow for a reverse bias voltage and will display an exponential increasing current for a forward bias. This result in a rectifying contact.
2. If $J \ll J_0$, the junction readily passes current for both signs of the applied voltage. In this cases equation 4.1 can be expanded to yield

$$V \cong \left(\frac{nKT}{J_0 q} \right) J \quad 4.3$$

This equation is linear in J and is Ohms law.

3. If $J \cong J_0$ i.e. if J and J_0 are comparable, then the J-V curve is neither rectifying nor Ohmic but symmetry.

J_0 can be obtained experimentally by extrapolating linear part of the log J versus V plot to the log J axis at a small forward bias. The intersection of this line with log J axis gives J_0 . Once J_0 is obtained, it is possible to calculate the barrier height ϕ_b and the ideality factor n from equation 4.1 and 4.2.

4.3 Impedance Spectroscopy

Impedance Spectroscopy is a relatively new and powerful technique for characterizing materials and their interface with the electronically conducting electrodes [22]. To measure

impedance one can do by applying voltage to the electrode interface and measuring the amplitude and the phase shift of the resulting current in the frequency domain. Impedance spectroscopy has been used to study dielectric and electrical properties of polymers [28,29-32].

Impedance spectroscopy method is useful to know more about the direct correlation between the response of a real system and an idealized model circuit. The important idea in the modeling studies is to match experimental impedance results with the impedance of ideal resistor and capacitor equivalent circuit [33].

The model circuit contains only a capacitor and a resistor, which described the dissipative components of the dielectric response and the storage components of the dielectric material.

Assuming a parallel circuit made of a capacitor and a resistor as shown in the **fig. 4.4** below, to see a simple model.

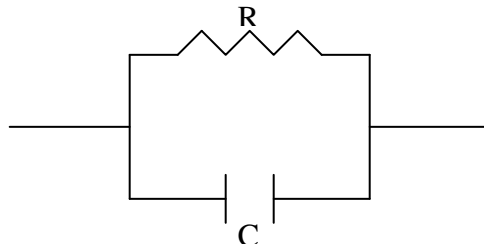


Fig. 4.4 Parallel RC circuits

The impedance for the above RC circuit is given by equation 4.4

$$Z = \frac{R}{1 + j\omega CR} = \frac{R}{1 + \omega^2 R^2 C^2} - j \frac{R^2 \omega C}{1 + \omega^2 C^2 R^2}, \quad 4.4$$

where j is the imaginary number defined by $\sqrt{-1}$ and ω is the frequency. Thus from equation 4.4 real and imaginary parts are separated as:

$$\text{Re}(Z) = \frac{R}{1 + \omega^2 R^2 C^2}, \quad 4.5a$$

and

$$-\text{Im}(Z) = \frac{R^2 \omega C}{1 + \omega^2 R^2 C^2} \quad 4.5b$$

The Cole – Cole plot of this circuit in this ideal form will be a semicircle whose center lies on the $\text{Re}(Z)$ axis as shown in **fig. 4.5** below [34].

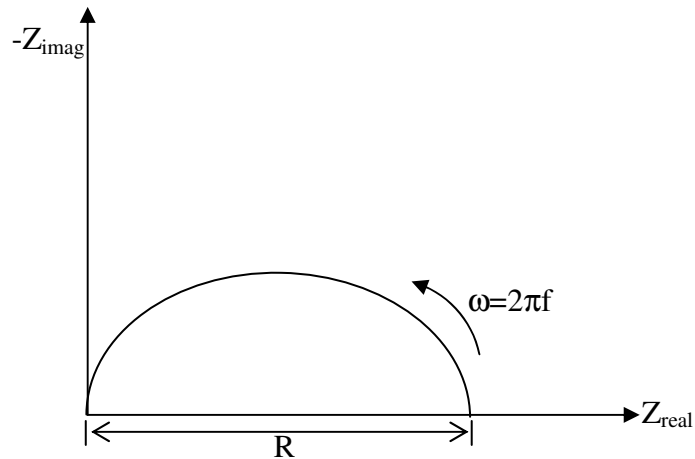


Fig.4.5 Cole-Cole plot of parallel RC circuit

If there is a contact resistance R_C in series with the RC parallel circuit the impedance given by equation 4.6 becomes

$$Z = R_C + \frac{R}{1 + j\omega RC} \quad 4.6$$

Whose Cole-Cole plot is as shown in the **fig. 4.6b** below

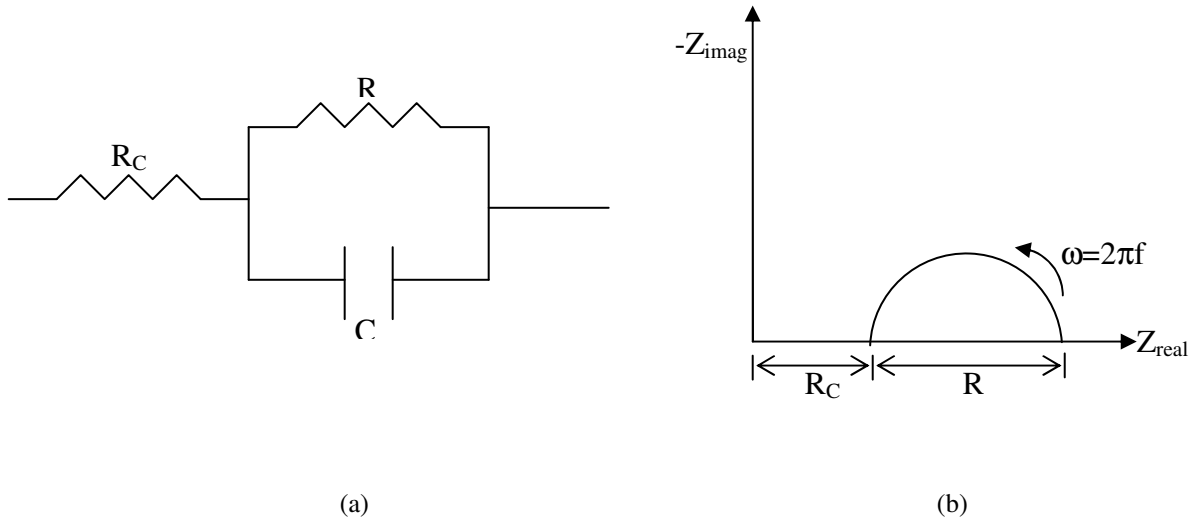


Fig.4.6 Circuit for a contact resistance R_c connected in series with parallel RC circuit (a) and its Cole-Cole plot (b)

The circuit model represented by the above **fig. 4.6** is an equivalent circuit model for a metal–semiconductor junction in which the depletion region accounts for the observed capacitance and resistance and the resistivity and the contact resistance accounts for the resistance of connecting wires for the apparatus used to measure the complex impedance characteristics.

Another model which is equivalent to a metal–insulator–semiconductor device can be obtained by considering two parallel RC circuits in series with R_C as shown in the **fig. 4.7** below.

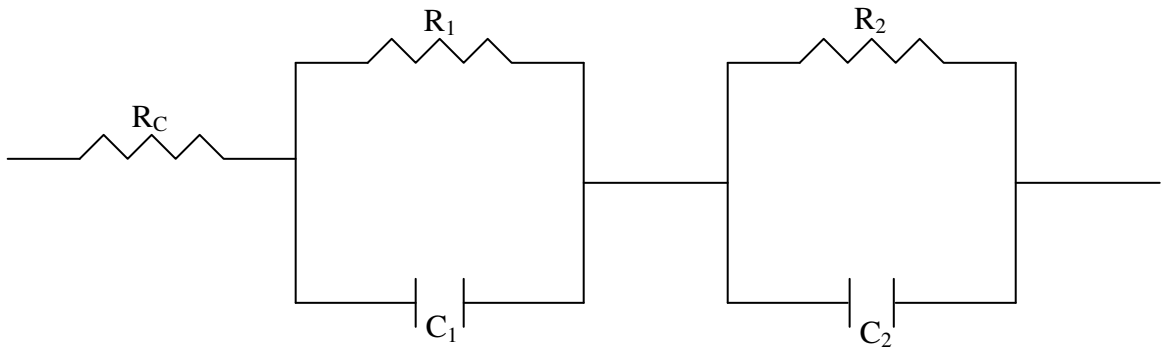


Fig.4.7 An equivalent RC circuit of metal-insulator-semiconductor device.

The complex impedance of the above circuit is given by

$$Z = R_C + \frac{R_1}{1 + j\omega R_1 C_1} + \frac{R_2}{1 + j\omega R_2 C_2} \quad 4.7$$

Here R_1 and C_1 represent the interfacial insulating thin layer, R_2 , and C_2 account for the depletion region. The Cole–Cole plot for such a model is shown in **fig.** 4.8 below.

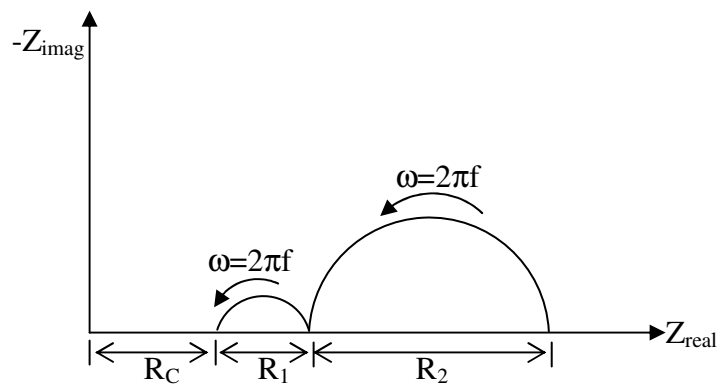


Fig.4.8 Idealized Cole-Cole plots for the circuit shown in **fig.** 4.7.

Many reports reveal the existence of an insulating interfacial layer between conjugated polymers doped with large anions and reactive metals, yielding two partially overlapping semicircles in a Cole-Cole plot [29-32].

4.4 capacitance-Voltage Relation

The relationship between capacitance and voltage is given by

$$\frac{1}{C^2} = \frac{2 \left[V_{bi} - V - \frac{KT}{q} \right]}{q \epsilon_0 \epsilon_s A_D^2 N_A} \quad 4.8$$

$$N_A = \frac{-2[\Delta V]}{q \epsilon_0 \epsilon_s A_D^2 \Delta \left[\frac{1}{C^2} \right]} \quad 4.9$$

where C is the capacitance, V_{bi} is the built in potential ϵ_s is the polymer dielectric constant, ϵ_0 is the permittivity in Vacuum, V is the applied Voltage, q is elementary charge A_D is the diode active area $\frac{KT}{q}$ is thermal Voltage at 300K and N_A is the doping concentration. The dielectric constant is here assumed to be 3[35].

The accuracy of Capacitance-Voltage (C-V) measurements depends on the frequency of the capacitance measurements. Higher frequency measurements are desired for accurate evaluation of the capacitance [36].

To find the depletion width, W, we can use the formula below

$$W^2 = \frac{2\epsilon_0\epsilon_s}{qN_A} \left(V_{bi} - V - \frac{KT}{q} \right) \quad 4.10$$

Where the term $\frac{KT}{q}$ arises from the contribution of the mobile holes to the electric fields. V_{bi} is the built-in potential, ϵ_s is the dielectric constant of the polymer, V is the applied voltage and N_A is the doping concentration.

5. Experiment

5.1 Absorption Spectrum Measurement

A 5mg solid form of the polymer was dissolved in 1 ml chloroform (CH_3Cl) to give a solution of the polymer with a concentration of 5mg/ml, which was used for absorption spectra, current-voltage, capacitance-voltage, and impedance spectroscopy measurements.

For optical absorption measurement, using a spinner with a remote control system, thin films of the polymer were spin coated on clean glass substrate at a rate of 6000rpm yielding a uniform, high quality reddish solid films of about 200-300nm thickness. The spin-coated substrate was then placed in the sample holder of PERKIN ELMER λ 19UV/VIS/NIR Spectrophotometer. With the help of ultra-violet computer spectroscopy software, UVCSS, the absorption spectrum was obtained, see **fig. 6.1**.

5.2 Current-Voltage Measurement

About two-third of the transparent conducting ITO (indium tin oxide) on glass was covered with photo-resist and the exposed ITO was etched with a mixture of concentrated Hydrochloric acid (HCl), Nitric acid (HNO_3), and water (H_2O) by the ratio of 48:4:48 in volume, respectively. The etched portion of the ITO/Glass provided a region convenient for electrical contacts to the aluminum layer deposited later. The photo-resist was removed using acetone, and then the surface was washed with detergents and distilled water, and rinsed with ethanol, see **fig. 5.1b** below.

Using a spinner with a remote control system, ITO/Glass substrate was spin coated with the polymer chloroform solution of 5mg/ml concentration at the rate of 6000rpm yielding uniform layer, see **fig. 5.1c** below. At this stage the polymer covers the whole area. For electrical contacts, part of the polymer from the etched part (pure glass) and the ITO part were cleaned with chloroform to obtain the structure shown in **fig. 5.1d** below that is ready for the deposition of aluminum.

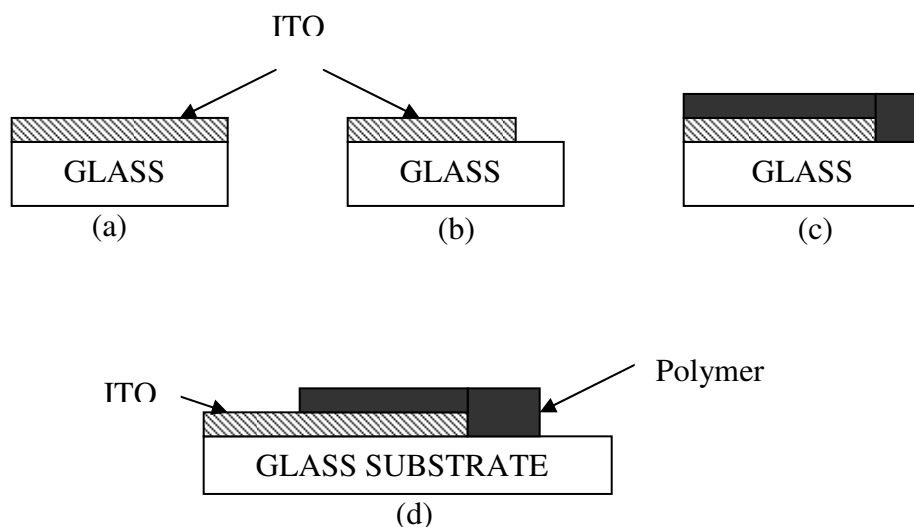


Fig.5.1 Preliminary steps in preparing the device.

Using Edwards Auto 306 Vacuum evaporator, aluminum which is a low work function metal, was evaporated at a pressure of 1×10^{-7} Torr on the polymer-ITO-glass substrate to get the sandwich structure of Al/poly[3-(2'-pentyloxy-5'-(1'''-oxoocty)phenyl)thiophene]/ITO, see **fig. 5.2** below.

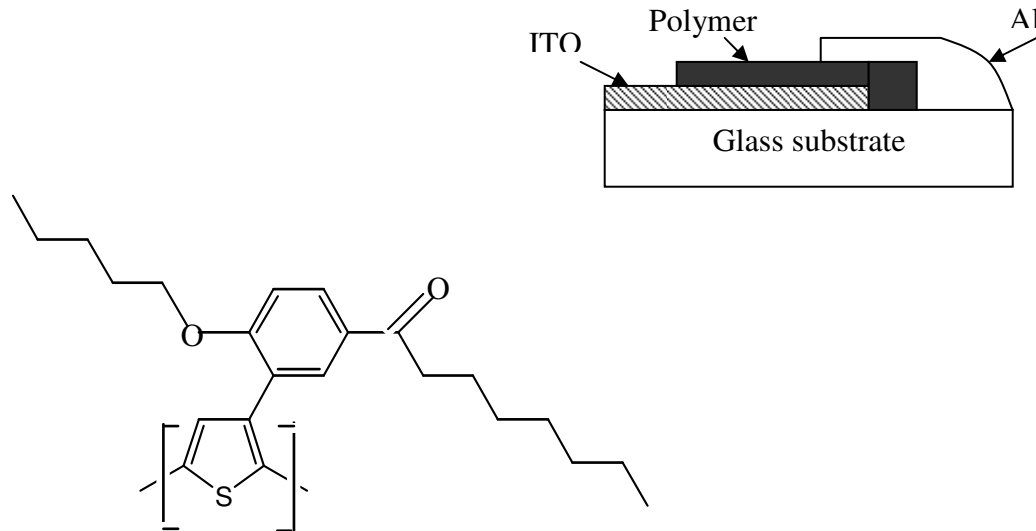


Fig. 5.2 Chemical structure of the polymer and the sandwich Al/poly[3-(2'-pentyloxy-5'-(1'''-oxoocty)phenyl)thiophene]/ITO-glass diode

The active area was about 4mm². The Al/poly[3-(2'-pentyloxy-5'-(1'''-oxoocty)phenyl)thiophene]/ITO sandwich structure shown in **fig. 5.2** above provides a means for current-voltage, capacitance-voltage and also impedance measurements. The diode was forward biased when the aluminum electrode was connected to a negative terminal of the voltage source so that current always flows from the Al to poly[3-(2'-pentyloxy-5'-(1'''-oxoocty)phenyl) thiophene] to ITO.

Current-voltage characteristics were measured with the HP 4140B together with the HP 16055A test fixture. The applied voltage was scanned between -3V and 3V.

5.3 Complex Impedance Measurement

Impedance Spectroscopy was measured with HP 4192A Low Frequency Impedance Analyzer together with a HP 16047A test fixture. The bias voltage applied to the sample ranged between -3V and 3V, in steps of 2V. For every bias voltage used, a sinusoidal oscillation voltage of $V_{\text{rms}} = 10\text{mV}$ was applied. The frequency was scanned between 5Hz and 10^6Hz for each bias.

5.4 Capacitance-Voltage Measurement

Capacitance was measured with the help of HP 4192A Low Frequency Impedance Analyzer together with a HP 16047A test fixture. The bias voltages applied to the sample ranges from -2V to 1V in steps of 0.1V at a frequency of 300 Hz see **fig. 6.4** below.

6. Results And Discussion

6.1 Absorption Spectrum

The band gap is important for the optical properties of the material, and it will affect the energy of light absorbed by the material as well as light emitted from the material. For conjugated polymers typical bands gaps may be around 1eV - 4 eV, which will place optical processes of the polymer in an optical wavelength window of 300nm to 700 nm [37].

The absorption spectrum of poly[3-2'-pentyloxy-5'-(1'''-oxoocty)phenyl]thiophene] polymer is shown in **fig. 6.1** below. It shows that the interband optical transition from valence band (π) to conduction band (π^*) lies is at about a wavelength of 612nm. From the relation of quantum theory of light, $E_g = \frac{hc}{\lambda}$, the band gap of the polymer is 2.02eV. This energy corresponds to the difference in energy scale between the Lowest Unoccupied Molecular Orbital (LUMO) and the Highest Occupied Molecular Orbital (HOMO). The above value confirms that the polymer is a semiconductor.

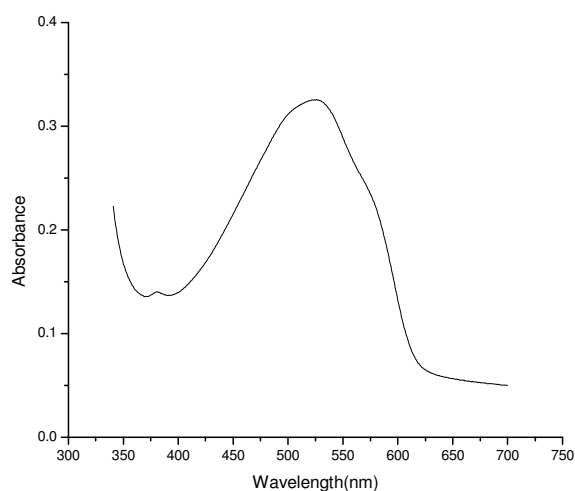


Fig. 6.1 Absorption spectrum of poly[3-(2'-pentyloxy-5'-(1'''-oxoocty)phenyl)thiophene].

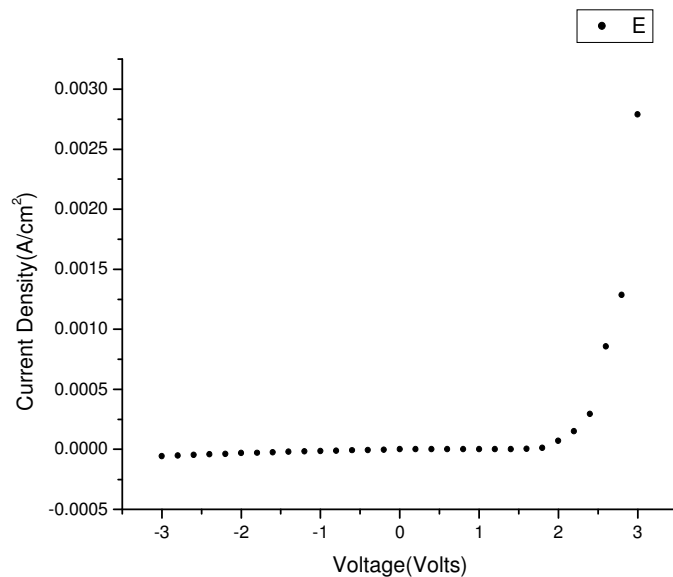
6.2 Current-Voltage Characteristics

The current-voltage (I-V) characteristics at room temperature in the dark of Al/poly[3-(2'-pentyloxy-5'-(1'''-oxoocty)phenyl)thiophene]/ITO sandwich structure is asymmetric and non-ohmic as shown in the **fig. 6.2a** below. There is also an exponentially increasing region at a forward voltage, but in the case of reverse bias voltage, the Schottky junction becomes highly resistive.

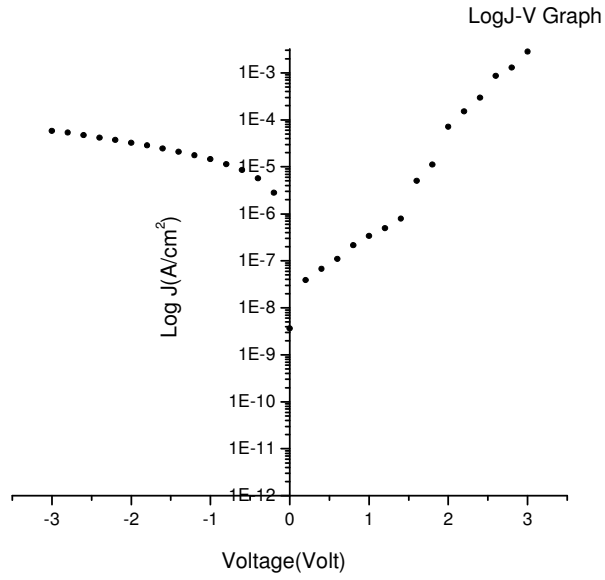
A semi-logarithmic plot of the forward current density (J) versus the applied voltage (V) shows that the forward current increases exponential from 1.8V to 2.6V, see **fig. 6.2b** below. This exponential dependence can be attributed to a formation of the depletion region near the Al/poly[3-(2'-pentyloxy-5'-(1'''-oxoocty)phenyl)thiophene] interface.

We note that, p-type semiconductor forms a rectifying barrier at the interface when the work function of the metal is smaller than that of the semiconductor. So that the polymer behaves as a p-type semiconductor.

The reverse saturation current density, J_0 , is found from the $\log J$ verses V curve by taking the intercept of the linear plot of $\log (J)$ verses V curve with $V = 0$ axis. It is found to be $2.3 \times 10^{-8} \text{ A/cm}^2$. By using the above value and the room temperature in absolute value the potential barrier, ϕ_b , is calculated to be 0.82 eV using equation 4.2.



(a)



(b)

Fig. 6.2 (a) Current density (J)-Voltage (V) characteristics, (b) logJ-V for poly[3-(2'-pentyloxy-5'-(1'''-oxooctyl)phenyl)thiophene]

The slope of the logarithmic plot is related to the quality factor n through the relation

$$\frac{1}{n} = \frac{KT}{q} \frac{\Delta \ln J}{\Delta V} \quad 6.1$$

With the help of equation 6.1, n is found to be 2.89. If the value of ideality factor (n) is one, then the Schottky barrier is ideal, whereas for higher values e.g. ideality factor $n \geq 2$ a midgap recombination of electrons and holes occurs.

Table 6.1 Parameters extracted from **fig 6.2**

$J_0(\text{A/cm}^2)$	$\phi_b(\text{eV})$	n	γ
2.3×10^{-8}	0.82	2.89	48.9

The rectification ratio for the polymer can also be obtained from the $\log(J) - V$ curve by considering the current at the two extreme biasing voltages (-3V and 3V). From this consideration the rectification ratio (γ) is found to be about 48.9.

6.3 Complex Impedance Analysis

Complex Impedance Spectroscopy (IS) is a powerful method of characterizing the electrical properties of materials and their interface with conducting electrodes. Such as the Schottky junction and the bulk resistance. The impedance spectroscopy results as a function of frequency and selected applied voltage in the forward and reverse bias, as shown in the **fig. 6.3a** below.

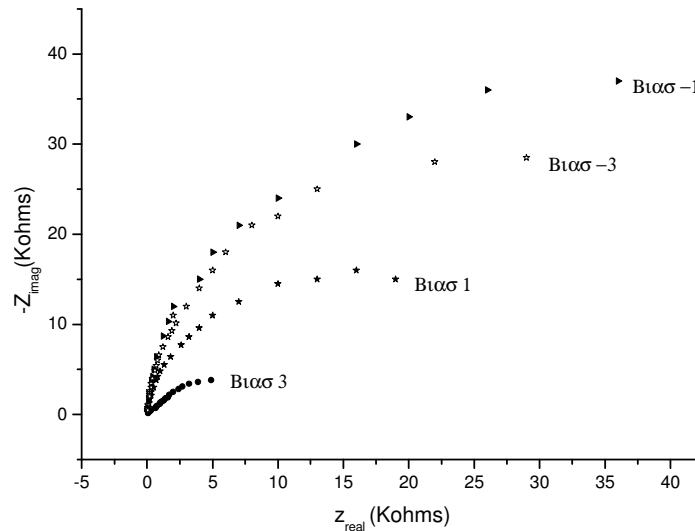


Fig. 6.3a Cole-Cole plot of Al/poly[3-(2'-pentylloxy-5'-(1'''-oxooctyl)phenyl) thiophene]/ITO sandwich structure.

The resistance of the depletion region and the corresponding depletion width decreases with increasing bias voltage. The impedance spectra consist of part of a single semicircle whose diameter corresponds to the resistance of the depletion region for the corresponding bias voltage. These semicircles are bias voltage dependent. For complex impedance spectra of sandwich structure for (Al/poly[3-(2'-pentyloxy-5'-(1''-oxoocty)phenyl)thiophene]/ITO), can be modeled by an equivalent circuit consisting of one parallel RC circuit in series with the contact resistance R_C . The contact resistance is the distance from the origin to the intersection of the semicircle with the real axis of the impedance plot corresponding to the highest frequency. The relation $-Z_{imag} = (\omega C)^{-1}$ is used to determine the value of the capacitance.

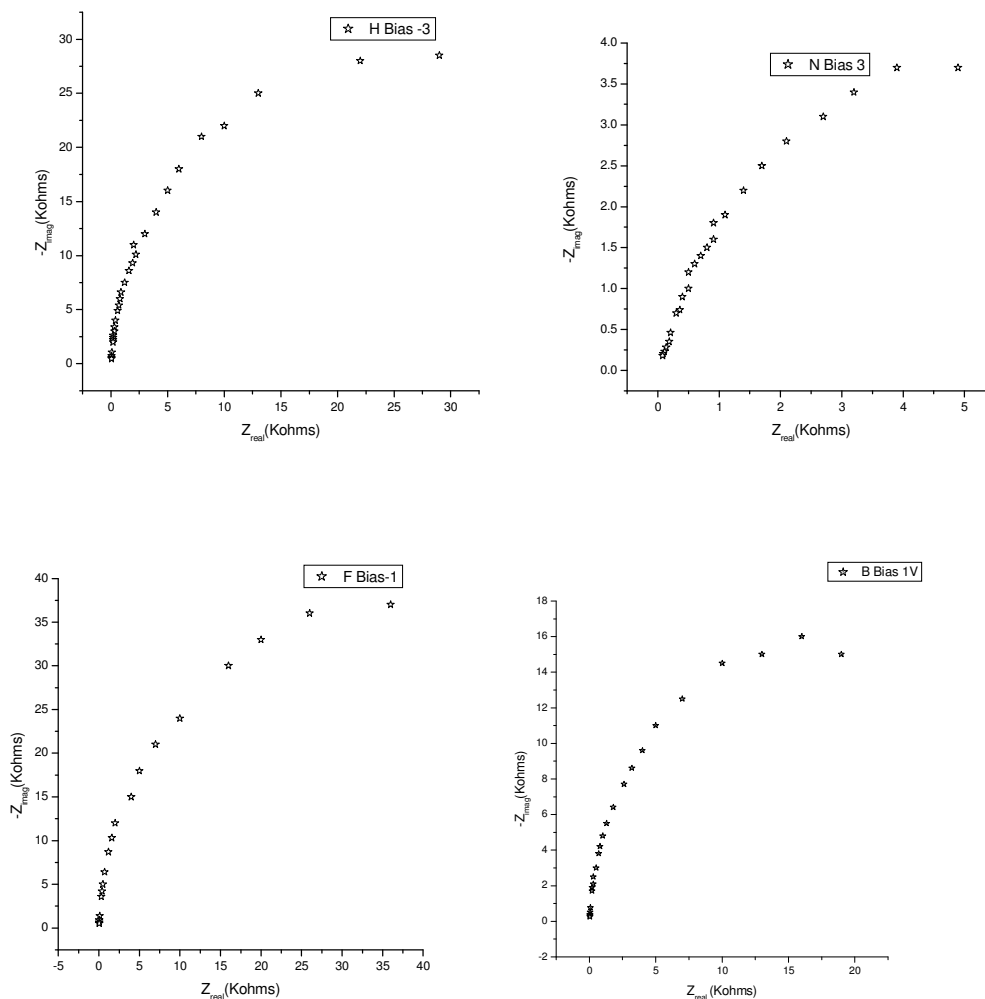


Fig. 6.3b Cole-Cole plots of different biasing voltage.

The above **fig. 6.3b** shows the IS results of the interface between Al/poly[3-(2'-pentyloxy-5'-(1'''-oxooctyl)phenyl)thiophene]. For each curve, the frequency increases in traversing from right to left. For each of the -3V and -1V reverse bias and 1V and 3V forward bias voltages, on to which a sinusoidal oscillating voltage of $V_{rms}=10mV$ is added, the frequency ranges between 5Hz to 10^6 Hz.

The Cole-Cole plot shown in **fig. 6.3** and the current-voltage characteristics shown in **fig. 6.2** are very consistent. For forward bias voltage the current is very high. The impedance curve shows less resistance (small semicircle) for forward bias voltage. The parameters obtained from the Cole-Cole of **fig 6.3** are listed in Table 6.2.

Table 6.2 parameter obtained from **fig. 6.3**

$V_b(V)$	$R_C(\text{Ohms})$	$R (\text{Kohms})$	$C (\text{nF/cm}^2)$
-3	80	58	228
-1	80	76	176
1	80	32	310
3	80	8	1650

where R_C and R are series and depletion region resistance, respectively. The negative values of V_b indicate reverse bias voltage.

6.4 Capacitance-Voltage Characteristics

When a small ac voltage is superimposed up on a dc bias, charge of one sign is induced on the metal surface and charge of the opposite sign in the semiconductor.

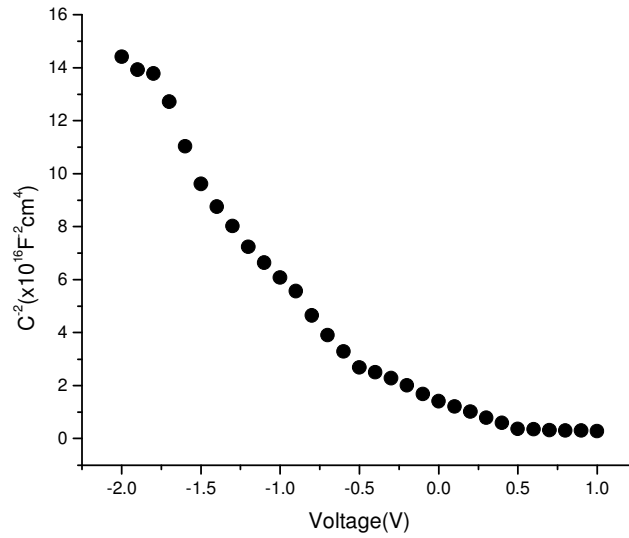


Fig. 6.4a The graph of C^{-2} versus V for poly[3-(2'-pentyloxy-5'-(1'''-oxooctyl)phenyl)thiophene]

From the **fig.** 6.4a above the built in potential, V_{bi} , is obtained from the intercept of the linear plot of C^{-2} versus V curve see **fig.** 6.4b below. From the intercept V_{bi} is obtained to be 0.61 V and also the doping concentration, N_A , calculated from the slope of the graph is found to be $2.3 \times 10^{16} \text{ cm}^{-3}$. Finally using dopant concentration (N_A) and the built-in potential (V_{bi}), the depletion width is found to be 234 \AA .

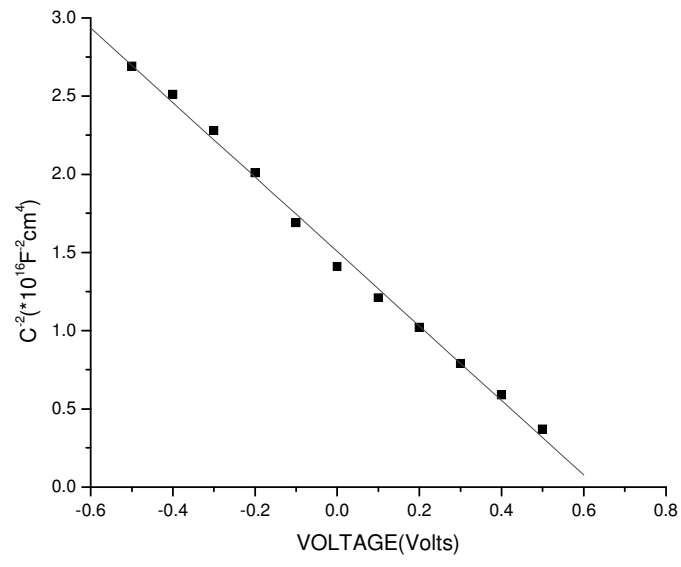


Fig. 6.4b Linear fit for the selected region of the C^2 -V plot.

7. Conclusion

In this research, we studied the electrical properties of the sandwich structure of Al/poly[3-(2'-pentyloxy-5'-(1'''-oxoocty)phenyl)thiophene]/ITO prepared in the laboratory here locally. In the sandwich structure poly[3-(2'-pentyloxy-5'-(1'''-oxoocty)phenyl)thiophene] is serving as an active semiconducting material in contact with a low work function, aluminum.

The absorption spectrum result shows that the energy gap of poly[3-(2'-pentyloxy-5'-(1'''-oxoocty)phenyl)thiophene] is 2.02eV. This value confirms that poly[3-(2'-pentyloxy-5'-(1'''-oxoocty)phenyl)thiophene] is an organic semiconductor.

The thermionic emission equation has been applied in order to interpret the J-V characteristics of the diode. The J-V measurement on Al/poly[3-(2'-pentyloxy-5'-(1'''-oxoocty)phenyl)thiophene]/ITO sandwich structure shows a Schottky barrier type diode with a rectification ratio of 48.9 at $\pm 3V$ and an ideality factor 2.89. The plot of $(C/A)^{-2}$ vs. V does not yield a straight line except in a very narrow voltage range, between -0.6V and 0.6V. This may be caused by a variable dopant concentration. The linear relationship of C^{-2} versus V curve in the low voltage range implies the absence of interfacial insulating layer between the metal and the semiconductor. Taking the data in the range between -0.6V and 0.6V, and approximating this with a linear function gives the built in voltage for poly[3-(2'-pentyloxy-5'-(1'''-oxoocty)phenyl) thiophene] diodes to be 0.61V. The dopant concentration obtained from the slope is $2.3 \times 10^{16} \text{cm}^{-3}$.

The complex impedance curves at different bias voltage show that the impedance of the depletion region are bias-voltage dependent. A single semicircle, modeled as one parallel RC equivalent circuit verifies Al/poly[3-(2'-pentylloxy-5'-(1'''-oxoocty)phenyl)thiophene]/ITO junction can be viewed as a metal- semiconductor (MS) contact.

Such electrical properties of junctions between Al and the polymer suggest that poly[3-(2'-pentylloxy-5'-(1'''-oxoocty)phenyl)thiophene] may manifest some results in its photovoltaic properties. Hence further investigations must do to find out these properties in the future.

8. References

- [1] L. H. Spirling, *Introduction to physical polymer Science*, John Wiley and Sons, Inc. New York, 1986.
- [2] Yu. Lu, *Solitons and Polarons in Conducting polymers*, World Scientific Publishing Co. Pt, Ltd., (1988).
- [3] C. K. Chiang, C. R. Fincher, J. Y. W. Park, A. J. Heeger, H. Shirakawa, E. J. Louis, S. C. Gau, and A. G. MacDiarmid, *Phys., Rev. Lett.* **39** (1997), 1098-1101.
- [4] J. Burroughes, D. D. C. Bradley, A. R. Brown, R. N. Marks, K. MacKay, R. H. Friend, P. L. Burns, and A. B. Holmes, *Nature* **347** (1997), 539-541.
- [5] A. J. Heeger, *Solid State, Commun.* **107** (1998), 673-679.
- [6] H. Sninghaus, N. Tessler, and R. H. Friend, *Science* **280** (1998), 1741-1744.
- [7] H. Kobayashi, S. Kanbe, S. Seki, H. Kiguchi, M. Kimura, I. Yudasaka, S. Miyashita, T. Shimoda, C. R. Towns, J. H. Burroughes, and R. H. Friend, *Synth. Met* **111** (2000), 125-128.
- [8] D. Lochun, M. Kilitziraki, D. Harrison, and I. Samuel, *Smart mater. Struct.* **10** (2001), 650-656.
- [9] F. Hide, M. A. Diazgarcia, B. J. Schwartz, M. R. Andersson, Q. B. Pei, and A. J. Heeger, A new class of Solid-State lasers materials, *Science* **273** (1996), 1833-1836.
- [10] N. Tessler, G. J. Dento, and R. H. Friend, *Nature* **382** (1996), 65-67.
- [11] P. Dyreklev, M. Berggren, O. Inganas, M. R. Andersson, O. Wennerstrom and T. Hjertberg, *Adv., Mat.* **7** (1995), 43.
- [12] M. Granstrom, M. Berggren, D. Pade, O. Inganas, M. R. Andersson, T. Hjertberg and O. Wennerstrom, *Supramolecular Science* **4** (1997), 27.

- [13] Bantikassegn Workalemahu, PhD Dissertation, ISBN 91-7871-803-1, Linkoping University, Sweden, 1996.
- [14] R. E. Peierls, *Quantum theory of Solids*, Oxford University press, London, (1955).
- [15] Ashcroft and Mermin, *Solid State Physics* Saunders College publishing New York, (1976).
- [16] M. J. Rice, *Phys., Lett. A* **71** (1979) 152.
- [17] W. P. Su, J. R. Schrieffer and A. J. Heeger, *phys. Rev. Lett.* **42** (1979) 1698.
- [18] Mats Fahlman, PhD Dissertation, ISBN 91-7871-625-x, Linkoping University, Sweden, 1995.
- [19] J. M. Andre, J. Delhalle, and J. L. Bredas, *Quantum Chemistry Aided Design of Organic Polymers World Scientific*, Singapore, (1991).
- [20] P. Gomes da Costa, R. G. Dandrea, and E. M. Conwell, *Phys.Rev. B* **47** (1993), 1800.
- [21] N. F. Mott and E. A. Davis, *Electronic Processing Non-Crystalline Materials*, Clarendon press, Oxford, (1979).
- [22] A. K. Jonscher, Chelsea Dielectric presses Limited, London, (1983).
- [23] Bantikassegn Workalemahu, *Organic semiconductors and Thin Film Devices*, 6th college on Thin Film Technology July 24-August 4, 2000.
- [24] E. H. Rhoderick and R. H. Williams, *Metal-Semiconductor Contacts*, 2nd ed., Clarendon, Oxford, 1988.
- [25] S. M. Sze, *Physics of Semiconductor Devices*, Wiley, New York, 1981.
- [26] H. Tomotawa, F. Braun, S. Phillips, A. J. Heeger and H. Kroemer, *Synth. Met.* **22** (1987) 63.
- [27] H. Koezuka and S. Etoh, *J. Appl. Phys.*, **54** (1983), 2511.
- [28] W. Bantikassegn and O. Inganas, *thin Solid Films*, **293** (1997), 138.
- [29] M. D. de Leeuw and E. J. Lous, *Synth. Met.* **65** (1994), 45.

- [30] S. Kary, W. Riess, V. Dyakonov and M. Schwoerer, *Synth. Met.* **54** (1993), 427.
- [31] W. Bantikassegn and O. Inganas, *Synth. Met.* **87** (1997), 5.
- [32] I. H. Campbell, D. L. Smith and J. P. Ferraris, *Appl. Phys. Lett.* **66** (22) (1995), 3030.
- [33] S. R. Macdonald, ed., *Impedance Spectroscopy Emphasizing Solid Materials and Systems*, John Wiley and Sons, New York, (1987).
- [34] K. S. Cole and R. H. Cole, *J. Chem. Phys.* **9** (1941), 341.
- [35] A. Assadi, C. Svensson, M. Willander and O. Inganas, *J. Appl. Phys.* **72** (1992), 2900-2906.
- [36] A. Moghaddam, PhD Dissertation, ISBN 91-7871-106-1, Linkoping University, Sweden, 1993.
- [37] M. Theander, W. Mammo, T. Olinga, M. Svensson, M. R. Andersson, and O. Inganas, *J. Phys. Chem. B* **133** (1999), 7771-7780.